



Thermophoretic separation of ultrafine particles in ferrofluids in thermal diffusion column under the effect of an MHD convection

E. Blums^{a,*}, S. Odenbach^b

^a*Institute of Physics, University of Latvia, Salaspils-1, LV-2169, Latvia*

^b*ZARM, University of Bremen, Am Fallturm, D-28359 Bremen, Germany*

Received 13 February 1999; received in revised form 15 June 1999

Abstract

The aim of the paper is to evaluate the Soret coefficient S_T of colloidal particles in ferrofluids from measurements of an unsteady particle separation in a flat thermodiffusion column. The column theory is modified taking into account MHD effects of thermal convection affected by a concentration buoyancy force. It is shown that the Hartmann effect, not only in hydrocarbon based colloids but also in ionic magnetic fluids of relatively high electric conductivity, does not influence significantly the particle separation dynamics. From measurements, positive values of S_T of surfacted particles in tetradecane based colloids are calculated. An anisotropy of the Soret effect in the presence of a uniform magnetic field is experimentally established. The obtained results agree qualitatively well with the authors hydrodynamic theory of particle thermomagnetophoresis. © 2000 Elsevier Science Ltd. All rights reserved.

Keywords: Magnetohydrodynamics; Mass transfer; Nanoscale

1. Introduction

Thermal diffusion may play an important role in some magnetic fluid and MHD technologies. For example, a change of directional solidification velocity in tin-bismuth alloy [1] has been observed. Recently, a high thermophoretic mobility of nanometer-scaled magnetite particles in ferrocolloids [2,3] have been measured. In nonisothermal conditions a remarkable redistribution of particle concentration in the colloid

takes place; therefore, a lowering of the long-term stability of ferrofluids in devices employing high temperature gradients may appear. Direct thermal diffusion measurements in liquid metals and in ferrocolloids are extremely difficult, since conventional interferometric and holographic methods are not available. Recently, it was shown [3] that the thermophoretic mobility of nanoparticles in magnetic colloids may be investigated by using an indirect method based on particle separation measurements in thermal diffusion columns. Usually, the Soret coefficient in molecular liquids is evaluated from the stationary level of particle separation (see, for example, [4]). In colloids, the Brownian diffusion coefficient of nanoparticles is significantly less than that of ordinary liquid mixtures

* Corresponding author. Tel.: +371-2-944-664; fax: +371-7-901-214.

E-mail address: eblums@tesla.sal.lv (E. Blums).

Nomenclature			
a	half-width of the channel	$z = z'/a$	vertical coordinate (oriented opposite to g)
B	induction of magnetic field		
$C = c/c_0$	non-dimensional particle concentration		
D	diffusion coefficient of colloidal particles	<i>Greek symbols</i>	
D_T	thermal diffusion coefficient	$\alpha = Ba(\sigma/\nu)^{1/2}$	Hartmann number
g	acceleration of gravity	$\alpha_T = S_T T$	non-dimensional thermal diffusion ratio
Gr	Grashoff number	$\beta_T = -\rho_0^{-1} \partial \rho / \partial T$	thermal expansion coefficient
$j = j'_z a / (c_0 D)$	particle flux density	$\beta_c = \rho_0^{-1} \partial \rho / \partial c$	solutorial expansion coefficient
$k = S_T \Delta T$	non-dimensional thermal diffusion parameter	δ_c	thickness of concentration buoyancy layer
L	length of the channel	$\varphi = c/\rho_p$	volume fraction of particles
$n = \delta_c/a$	non-dimensional concentration layer thickness	μ	magnetic permeability
Rz	vertical non-dimensional concentration gradient	μ_0	magnetic constant
$S_T = D_T/D$	Soret coefficient	ν	fluid viscosity
$Sc = \nu/D$	Schmidt number	ρ	density
$u = u_z(x)$	vertical convection velocity	σ	fluid electric conductivity
$U = ua/D$	convection velocity (non-dimensional)	$\tau = Dt/a^2$	non-dimensional time
$x = x'/a$	coordinate across the channel	<i>Subscripts</i>	
		0	initial
		T	temperature
		c	concentration

and the steady separation regime is reached in long time experiments of several days. Besides, the final result may be disturbed by many uncontrolled factors. In the present paper we describe an approximate column theory which allows evaluation of the Soret coefficient from the initial part of unsteady separation measurements. Since the density of the ferrite particles differs significantly from that of a carried liquid, the description of the convective flow in the column must not only consider the thermal but also the concentration buoyancy forces (the so called 'forgotten effect' [5]). To allow the possibility of analyzing separation measurements performed in the presence of an external magnetic field in our theory, the convection problem accounts also for a Hartmann effect. In the last section of the paper we present a review of our results on the magnetic Soret effect in hydrocarbon-based ferrofluids which are obtained from unsteady separation measurements.

2. Steady MHD convection in a thermal diffusion column

Let us consider a convective flow and a mass transfer in a thermal diffusion column consisting of a verti-

cal flat channel and upper and lower separation chambers. The channel walls $x' = \pm a$ have different temperatures $T(-a) = T_1$ and $T(a) = T_2$. Both, the height and the width of the channel significantly exceed the thickness of the gap $\delta = 2a$. Therefore, the convection in the channel may be considered in a one-dimensional approximation $u = u_z(x)$.

Steady convection in the presence of an uniform magnetic field B oriented normally to the vertical walls (along z) may be considered in classical Boussinesq approximation

$$\rho \nu \frac{d^2 u}{dx'^2} - \frac{dp}{dz'} - \sigma B^2 u - g(\rho - \rho_0) = 0. \quad (1)$$

Here dp/dz' is the vertical pressure gradient, ν and σ are the viscosity and the electric conductivity of the fluid, coordinate z' is directed opposite to the acceleration of gravity g . The third term in this equation reflects the MHD interaction due to an inductive electric current. The dependence of the ferrocolloids magnetization on temperature causes a transversal pressure gradient dp/dx' but it is assumed to be less than the critical one at which the thermomagnetic instability of convection may develop. (The transversal magnetization gradient is one of the reasons for a magnetic Soret effect of ferroparticles discussed below.) If the

magnetic field is oriented horizontally along the channel walls, the induced electric field does not affect convection velocity and a magnetostatic pressure gradient due to fluid magnetization also does not appear.

The colloids density ρ depends on temperature T as well on particle concentration c . In a linear approximation we may write:

$$\begin{aligned} \rho &= \rho_0 + \frac{\partial \rho}{\partial T_c}(T - T_0) + \frac{\partial \rho}{\partial c_T}(c - c_0) \\ &= \rho_0[1 - \beta_T(T - T_0) + \beta_c(c - c_0)]. \end{aligned} \quad (2)$$

Thus, the buoyancy force in Eq. (1) must be considered being dependent not only on temperature but also on the inhomogeneity of the particle concentration which develops during thermodiffusive transfer. The temperature distribution across the channel in a steady convection regime is linear.

$$T = T_0 + (T_2 - T_1)\frac{x'}{2a} = T_0 + \Delta T\frac{x'}{2a}. \quad (3)$$

The steady distribution of particle concentration, corresponding to a zero value of particle flux on impermeable channel walls given by

$$\begin{aligned} j'_x &= -D\frac{\partial c}{\partial x'} - D_T\frac{dT}{dx'}c = -D\left(\frac{\partial c}{\partial x'} + \frac{S_T\Delta T}{2a}c\right) \\ &= 0 \quad \text{at} \quad \frac{x'}{a} = \pm 1 \end{aligned} \quad (4)$$

in the initial stage of separation (where it is used that $c \ll 1$ in common magnetic fluids and that the vertical concentration gradient in the column is not yet developed) follows an exponential law

$$C = \frac{c}{c_0} = \frac{k}{\sinh k} \exp(-kx), \quad k = \frac{S_T\Delta T}{2}, \quad x = \frac{x'}{a}. \quad (5)$$

Here $S_T = D_T/D$ is the Soret coefficient, D and D_T are the Brownian and the thermal diffusion coefficients of the nanoparticles, respectively and k is the non-dimensional separation parameter. In conventional thermal diffusion column theories which are developed considering molecular liquids with $k \ll 1$, a linear dependence $C = 1 - kx$ is usually used instead of Eq. (5). In magnetic colloids the parameter k may reach significantly higher values $k \approx 1$ [2], therefore the exponential concentration profile (5) must be considered in the column theory. Taking into account the profiles (3) and (5), we obtain from profile (1) the following distribution of a vertical convection velocity across the channel $U = ua/D$ [6]:

$$\begin{aligned} U &= \frac{Gr_T Sc}{2a^2} \left(x - \frac{\sinh \alpha x}{\sinh \alpha} \right) \\ &\quad - \frac{Gr_c Sc}{(\alpha^2 - k^2)} \left[\left(\frac{1 - \frac{k}{\tanh k}}{1 - \frac{\tanh \alpha}{\alpha}} \right) \left(\frac{\cosh \alpha x}{\cosh \alpha} \right) \right. \\ &\quad \left. - \frac{\tanh \alpha}{\alpha} \right] + \frac{k \sinh \alpha x}{\sinh \alpha} + \frac{k \exp(-kx)}{\sinh k} - 1 \quad (6) \end{aligned}$$

Here $Gr_T = \beta_T \Delta T g a^3 / \nu^2$ and $Gr_c = \beta_c g c_0 a^3 / \nu^2$ are the thermal and the concentration Grashoff numbers, $Sc = \nu/D$ is the Schmidt number of colloidal particles and $\alpha = Ba\sqrt{\sigma/\rho\nu}$ is the Hartmann number. For small values of the thermal diffusion parameter $k \ll 1$ a simpler dependence which corresponds to an additive action of thermal and concentration buoyancy forces on free convection is valid:

$$U = \frac{(Gr_T + 2kGr_c)Sc}{2\alpha^2} \left(x - \frac{\sinh \alpha x}{\sinh \alpha} \right). \quad (7)$$

In the initial stage of the separation process the mean particle concentration in a channel may be considered being independent from the vertical coordinate and equal to $c = c_0$. Using this assumption, from Eq. (6) we obtain the vertical particle flux j'_z written in a non-dimensional form

$$\begin{aligned} j'_z &= \frac{j'_z a}{c_0 D} = \frac{1}{2} \int_{-1}^{+1} CU \, dx = \frac{k}{2 \sinh k} \int_{-1}^{+1} e^{-kx} U \, dx \\ &= \frac{Gr_T Sc}{2\alpha^2} \left[\frac{k}{(\alpha^2 - k^2)} \left(\frac{\alpha}{\tanh \alpha} - \frac{k}{\tanh k} \right) \right. \\ &\quad \left. - \frac{1}{\tanh k} + \frac{1}{k} \right] - \frac{Gr_c Sc}{(\alpha^2 - k^2)} \left\{ \frac{(1 - k/\tanh k)}{(1 - \tanh \alpha/\alpha)} \right. \\ &\quad \times \left[\frac{k}{(\alpha^2 - k^2)} \left(\frac{\alpha \tanh \alpha}{\tanh k} - k \right) - \frac{\tanh \alpha}{\alpha} \right] \\ &\quad \left. - \frac{k^2}{(\alpha^2 - k^2)} \left(\frac{\alpha}{\tanh \alpha} - \frac{k}{\tanh k} \right) + \frac{k}{\tanh k} - 1 \right\}. \end{aligned} \quad (8)$$

Fig. 1 represents this solution graphically. From Eq. (8) and Fig. 1a it is seen that in the case where the thermodiffusive transfer of particles across the channel does not affect the buoyancy force ($Gr_c = 0$) the direction of particle convective separation in the column depends on the sign of parameter k in a simple way. Particles which are moving toward increasing temperatures ($k < 0$) will be collected in the upper separation chamber of the column whereas positive

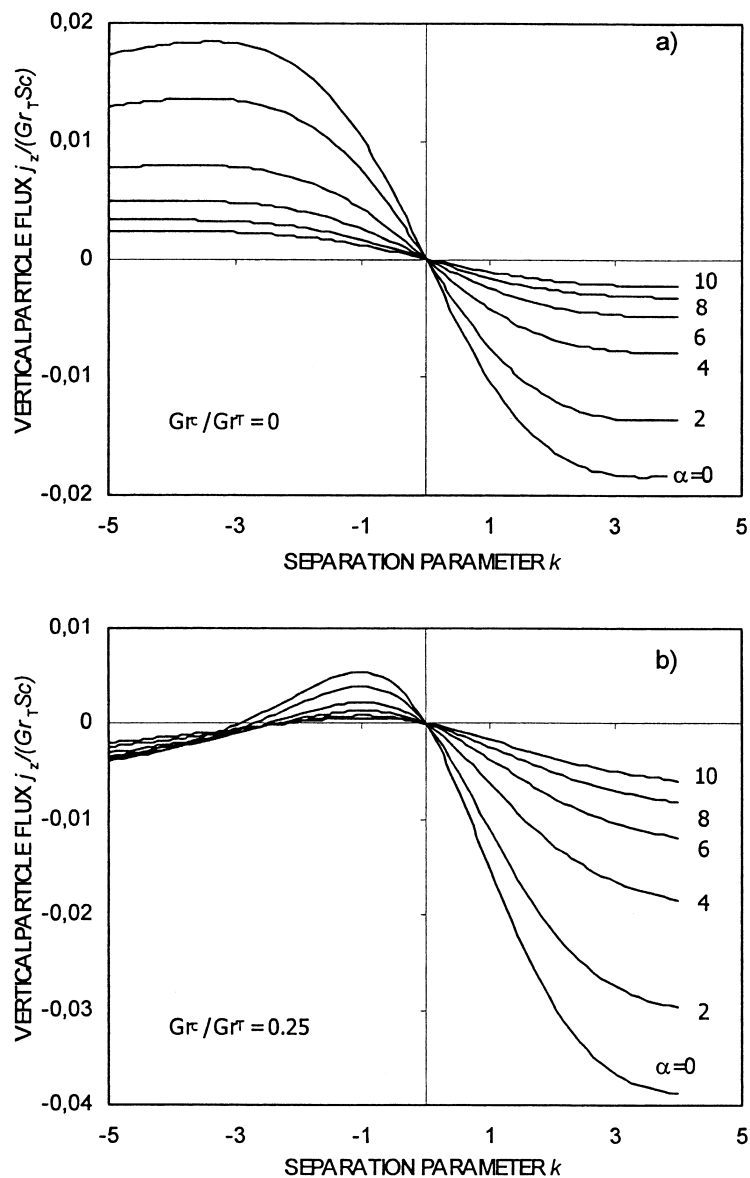


Fig. 1. Vertical particle flux $j_z/Gr_T Sc$ in a flat vertical channel in the presence of a transversal magnetic field $B = B_x = \text{const.}$ at various α , $Gr_c/Gr_T = 0$ (a) and $Gr_c/Gr_T = 0.25$ (b).

Soret coefficients will cause a rise of particle concentration in the lower chamber. Magnetohydrodynamic suppression of convection always causes a significant reduction of the particle separation intensity. If the concentration buoyancy force is taken into account, the situation is more complicated. The density of particles ρ_p in magnetic fluids, is significantly higher than that of a carrier liquid ρ_0 . Therefore, usually $Gr_c \gg 0$, and even at low thermal diffusion coeffi-

cients the concentration buoyancy force significantly affects both, the convection velocity and the vertical convective transfer of particles. From expression (8) and from results presented in Fig. 1b it follows that under the conditions of an intensive thermal diffusion, the convective particle flux may be directed in the direction of gravitational acceleration g independently of the sign of parameter k . The particle collection in the upper chamber is expected only in a relatively

narrow interval of negative values of the parameter k (for small k this interval is equal to approximately $0 > k > -Gr_T/2Gr_c$) when the thermogravitational mechanism of free convection in the channel still prevails. From the results presented in Fig. 1b we can see, that this interval of parameter k depends on the value of the Hartmann number α . Magnetohydrodynamic deformation of the convection profile causes an increase of probability to form a reverse convective flow under the action of a concentration buoyancy force.

3. Quasi-stationary convection during the formation of the concentration profile across the channel

The steady concentration profile (5) is valid only for narrow channels for times t larger than a transition time t_0 , $t > t_0 \approx a^2/D$. In the initial regime of particle separation, $t < t_0$, an unsteadiness of the concentration profile in Eqs. (1) and (2) has to be taken into account. To simplify the calculation in this regime, we will use an approximate profile [6]

$$\frac{c}{c_0} - 1 = \pm \frac{kn}{3 \mp kn} (n - 1 \mp x)^3, \quad n = \sqrt{12\tau},$$

$$\tau = \frac{Dt}{a^2},$$

which satisfies the equation of integral mass balance in the boundary layer. Here is $n = \delta_c/a$ with δ_c being the thickness of the concentration boundary layer near both walls. (The upper signs in Eq. (9) correspond to negative $x < 0$, the lower ones to positive x). This approximation is very close to concentration profiles of an exact solution of the unsteady diffusion equation. For example, from the exact solution it follows that at $\tau \ll 1$ the gradient of concentration at channel walls is equal to $c'_w = c_0 2\sqrt{\tau/\pi}$, whereas the approximate profile (9) gives a value of the coefficient in this ‘square root’ law equal to $2/\sqrt{3}$.

Let us consider for simplicity only one half of the channel, $x = 0-1$. For small $kn \ll 3$ the concentration profiles $C - 1$ near both channel walls are anti-symmetric, therefore $dp/dz' = 0$. The velocity profile for positive x is now given by:

1. if $|x| < n$:

$$\frac{U}{Gr_T Sc} = \frac{1}{2\alpha^2} \left[\left(x - \frac{\sinh \alpha x}{\sinh \alpha} \right) - S \left(\frac{n}{3} + \frac{2}{n\alpha^2} - \frac{2 \sinh n\alpha}{n^2 \alpha^3} \right) \frac{\sinh \alpha x}{\sinh \alpha} \right];$$

2. if $n \leq |x| \leq 1$:

$$\frac{U}{Gr_T Sc} = \frac{1}{2\alpha^2} \left\{ \left(x - \frac{\sinh \alpha x}{\sinh \alpha} \right) + S \left[\frac{2 \sinh \alpha(1-n) \cdot \cosh \alpha \cosh \alpha x}{n^2 \alpha^3 \cosh \alpha} - \left(\frac{n}{3} + \frac{2}{n\alpha^2} + \frac{2 \sinh \alpha(1-n) \cdot \cosh \alpha}{n^2 \alpha^3} \right) \times \frac{\sinh \alpha x}{\sinh \alpha} - \frac{(1-n-x)^3}{3n^2} - \frac{2(1-n-x)}{n^2 \alpha^3} \right] \right\}.$$

The corresponding mass flux for one-half of the channel is the following:

$$\frac{j_z}{kGr_T Sc} = -\frac{1}{6n^2 \alpha^3} \left\{ \left[\left(\frac{3n^2}{\alpha^2} + \frac{6}{\alpha^4} \right) - \frac{1}{\tanh \alpha} \left(\frac{n^3}{\alpha} + \frac{6n}{\alpha^3} \right) - \frac{6 \sinh \alpha(1-n)}{\alpha^4 \sinh \alpha} + \frac{n^4}{4} - \frac{n^5}{20} \right] - S \left[\frac{2 \sinh \alpha(1-n)}{n^2 \alpha^3 \sinh \alpha} \left(\frac{n^3}{\alpha} + \frac{6n}{\alpha^3} - \frac{6 \sinh \alpha n}{\alpha^4} \right) - \left(\frac{n}{3} + \frac{2}{n\alpha^2} \right) \times \left(\frac{3n^2}{\alpha^2} + \frac{6}{\alpha^4} - \frac{1}{\tanh \alpha} \times \left(\frac{n^3}{\alpha} + \frac{6n}{\alpha^3} \right) - \frac{6 \sinh \alpha(1-n)}{\alpha^4 \sinh \alpha} \right) - \frac{n^5}{21} - \frac{2n^3}{5\alpha^2} \right] \right\}.$$

For small Hartmann number values $\alpha \rightarrow 0$ a simpler solution instead of Eqs. (10a), (10b) and (11) is valid:

$$\frac{U}{Gr_T Sc} = \frac{1}{12} (x - x^3) + \frac{S}{2} \left[\frac{n^3}{60} x - \frac{1}{60n^2} (n - 1 + x)^5 \right],$$

$$\frac{j_z}{kGr_T Sc} = -\frac{1}{360} \left(n^3 - \frac{n^4}{2} + \frac{n^5}{14} \right) - \frac{5S}{360 \times 36} \left(n^5 - \frac{9}{25} n^6 \right)$$

Here $S = kGr_c/Gr_T$

Some unsteady convection velocity profiles which correspond to various τ at the initial stage of particle separation $Dt/a^2 < 1/12$, when the concentration boundary layer approximation (9) is valid, are shown in Fig. 2. Profiles are plotted in accordance with expressions (10a) and (10b) for $\alpha = 10$, the curves corre-

respond to equivalent positive (Fig. 2a) and negative (Fig. 2b) values of the thermal diffusion parameter $\pm S$. In colloids having positive Soret coefficients ($S > 0$), the particle transfer across the channel causes a monotonous increase of the convection velocity. In the presence of a strong magnetohydrodynamic interaction, $\alpha \gg 1$, the action of unsteady concentration buoyancy force is concentrated mainly in a thin fluid layer near the channel walls, as seen in Fig. 2. In electrically non-conducting fluids at $\alpha = 0$ the velocity changes take place not only near the walls but also in the central part of the channel. If particles are moving towards increasing temperature ($S < 0$), the concentration buoyancy force is directed opposite to the thermogravitation one. Therefore, non-monotonous velocity profiles develop during the formation of the concentration profile across the channel. Finally, reaching $\tau = \tau_0 \approx 1$, a reverse anti-symmetric velocity distribution develops which corresponds to the steady profile (6) (in the transition period $1/12 < \tau < \tau_0$ the velocity profiles may not be calculated because the boundary layer approximation and the profile (9) are no more valid).

The dependence of the vertical particle flux on time for various values of the fluid Hartmann number is shown in Fig. 3. If particles are transferred across the channel towards decreasing temperature ($S > 0$), the concentration buoyancy force causes an increase of the vertical particle flux; particles are collected in the lower chamber. If the values of S are negative, the particles are transferred upward in the initial period of time, but due to development of a concentration buoyancy force which now acts opposite to the thermogravita-

tion force, a monotonous reduction of particle flux takes place. When the regime of a reversed convection velocity near the channel walls is reached, the vertical mass flux turns to the opposite direction. Therefore, particles like in the previous case $S > 0$, are transferred again to the lower separation chamber. Finally, reaching $\tau = \tau_0$ there develops a steady particle flux (Eq. (8)) which corresponds to the velocity profile (Eq. (6)) of a stationary particle distribution across the channel. The magnetohydrodynamic suppression of convection velocity always causes a reduction of the intensity of particle separation in the nonstationary regime.

The non-monotonous velocity profiles of several stagnation points which develop at $S < 0$ (Fig. 2b) are obviously unstable. The loss of shear flow stability in the channel during the reversion of the convection velocity may significantly affect the dynamics of particle separation. It is also not clear, whether it is possible to observe the reversion of the particle flux or not. In our preliminary experiments we have observed that at negative Soret coefficients an oscillatory regime of particle separation in the channel may occur [2,7]. An unstable regime of separation is also observed in molecular liquids with $S_T < 0$ [8].

4. The limit of a steady regime of particle separation

The equations given in Sections 2 and 3 are valid only for channels of infinite height or for real thermal diffusion columns in the initial regime of particle separation. At durable separation a remarkable concen-

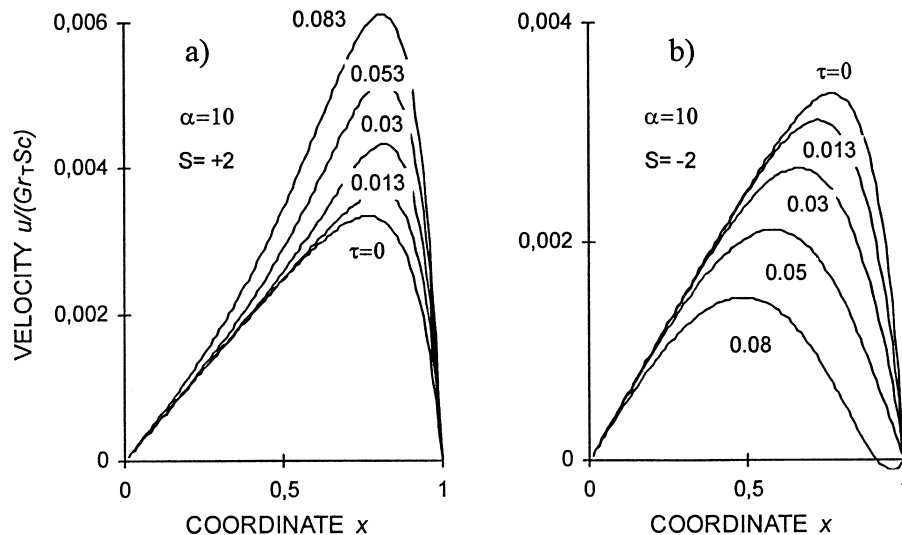


Fig. 2. The development of the convection velocity profiles across the channel in the presence of an uniform transversal magnetic field (only the part of the channel for positive x is shown, $\alpha = 10$, $S = +2$ (a) and $S = -2$ (b)).

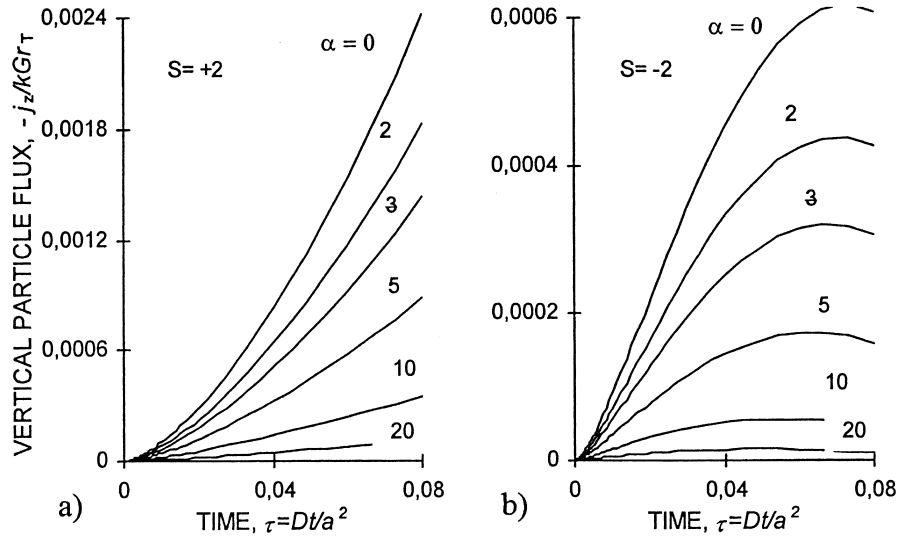


Fig. 3. The unsteady vertical particle flux in a flat thermal diffusion channel for various α , $S = +2$ (a) and $S = -2$ (b).

tration difference in the upper and lower separation chambers develops. The corresponding vertical concentration gradient in the channel affects both, the velocity as well as the concentration profile, across the channel. Instead of Eq. (5), the concentration profile $C = C(x)$ must now be calculated considering a convective mass transfer too. For low c_0 and small values of the thermal diffusion parameter k , when the separation term in Eq. (4) may be considered being constant, the mass conservation equation for a one-dimensional flow in the channel must be written in the form

$$U \frac{\partial C}{\partial x} = \frac{\partial^2 C}{\partial z^2} \tag{14}$$

The solution of Eqs. (1) and (14), considering Eqs. (3) and (4), for the steady asymptotic regime of separation $j_z = 0$ is now the following:

$$U = \frac{Gr_T Sc(1+S)}{2Q_1} (\sinh \beta_2 \sinh \beta_2 x - \sinh \beta_1 \sinh \beta_1 x) \tag{15}$$

$$C - 1 = -\frac{Gr_T(1+S)}{2Gr_c Q_1} (\beta_2^2 \sinh \beta_2 \sinh \beta_1 x - \beta_1^2 \sinh \beta_1 \sinh \beta_2 x) + x \tag{16}$$

with

$$S = \frac{2Q_1 Q_2}{Q_3} - 1 \tag{17}$$

and

$$Q_1 = \beta_1 \beta_2 (\beta_2 \cosh \beta_1 \sinh \beta_2 - \beta_1 \cosh \beta_2 \sinh \beta_1) \tag{18}$$

$$Q_2 = \sinh \beta_2 \left(\frac{\cosh \beta_1}{\beta_1} - \frac{\sinh \beta_1}{\beta_1^2} \right) - \sinh \beta_1 \left(\frac{\cosh \beta_2}{\beta_2} - \frac{\sinh \beta_2}{\beta_2^2} \right) \tag{19}$$

$$Q_3 = \beta_2^2 \sinh^2 \beta_2 \left(\frac{\sinh^2 \beta_1}{2\beta_1} - 1 \right) + \beta_1^2 \sinh^2 \beta_1 \left(\frac{\sinh^2 \beta_2}{2\beta_2} - 1 \right) - \frac{\alpha^2}{(\beta_1^2 - \beta_2^2)} (\beta_1 \sinh^2 \beta_2 \sinh^2 \beta_1 - \beta_2 \sinh^2 \beta_1 \sinh^2 \beta_2) \tag{20}$$

The coefficients β_1 and β_2 depend on the Hartmann number α and on steady vertical concentration gradient $Rz = Gr_c Sc (\partial C / \partial z)$:

1. if $Rz > 0$:

$$\beta_1 = \left[\left(\frac{\alpha^4}{4} + Rz \right)^{1/2} + \frac{\alpha^2}{2} \right]^{1/2}, \beta_2 = i \left[\left(\frac{\alpha^2}{2} + Rz \right)^{1/2} - \frac{\alpha^4}{4} \right]^{1/2} \quad (21)$$

2. if $Rz = -Rn$ is negative and $Rn < \alpha^4/4$:

$$\beta_1 = \left[\frac{\alpha^2}{2} + \left(\frac{\alpha^4}{4} - Rn \right)^{1/2} \right]^{1/2}, \beta_2 = i \left[\frac{\alpha^2}{2} - \left(\frac{\alpha^4}{4} - Rn \right)^{1/2} \right]^{1/2} \quad (22)$$

3. if $Rz = -Rn$ is negative and $Rn > \alpha^4/4$:

$$\beta_{1,2} = \frac{1}{2} \left[(2Rn^{1/2} + \alpha^2)^{1/2} \pm i(2Rn^{1/2} - \alpha^2)^{1/2} \right] \quad (23)$$

Fig. 4 represents some velocity and concentration profiles ($\alpha = 5$) which correspond to positive and negative Soret coefficients. It is seen that at negative S the change of direction of convection, expected in the previous section for flows without vertical concentration gradients, is not observed. The reason for that, obviously, is the non-monotonous character of concentration profile across the channel which is formed under the effect of different inlet concentrations of the upstream and downstream convective flows. The dependence of a steady limit of the vertical concen-

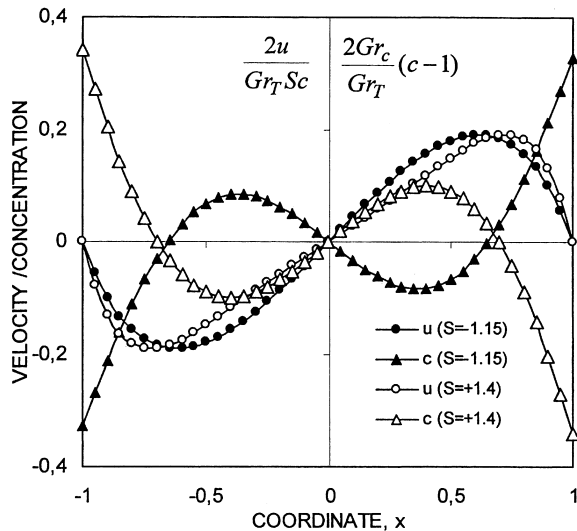


Fig. 4. Velocity (circles) and concentration (triangles) profiles at steady particle separation, $\alpha = 5$. Black points: $S = -1.15$, $Rz = 120$; white points: $S = +1.40$, $Rz = -155$.

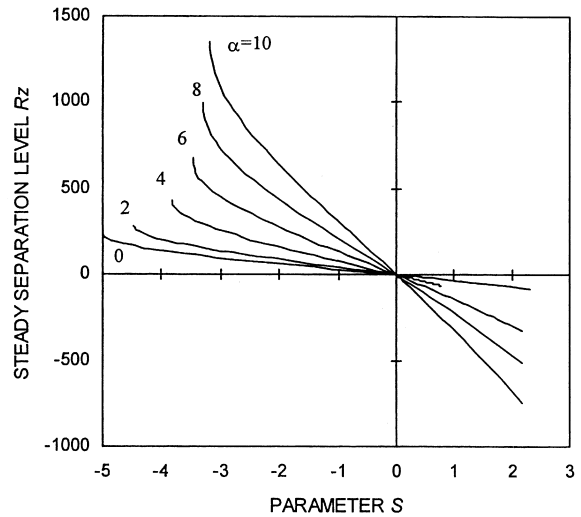


Fig. 5. Dependence of vertical concentration gradient Rz on parameter S in a steady regime of particle separation.

tration gradient on the Soret parameter S for various Hartmann numbers is plotted in Fig. 5. For non-conducting liquids at $\alpha \rightarrow 0$ the solutions (15) and (20) coincides with the results published by Ecenarro et al. [9]. In a region where $|S| < 2$ a relation

$$Rz = \frac{63S}{2} \quad (24)$$

is valid.

From the results presented in Fig. 5 it is seen, that in the presence of a magnetic field the coefficient in Eq. (24) monotonously increases. Thus, the magneto-hydrodynamic breaking of convection leads to an increase of the steady thermodiffusive separation limit in the column. In the region of negative Soret coefficients the curves presented in Fig. 5 are calculated until the shear stress of the flow at the channel walls reaches zero. In a zero field this happens at $S = -5$, for higher Hartmann numbers this limit monotonously decreases and for $\alpha = 10$ it reaches a value approximately equal to $S = -3$. This tendency of a lowering of the convection stability in the presence of strong MHD interaction is also observed in flows without vertical concentration gradients; only the corresponding S values are smaller (compare results presented in Figs. 3 and 5).

5. The dynamics of particle separation in a thermal diffusion column

The sketch of the thermal diffusion column used in

our experiments is shown in Fig. 6. The column consists of a vertical flat channel (a small gap $\delta = 2a$ between two plates of different temperatures T_1 and T_2) of a length $L/a \gg 1$ and two separation chambers of equivalent volumes V_c .

The convective vertical flux j_z in the channel causes a particle concentration change in the lower (c_l) and in the upper (c_u) chamber of the column:

$$\frac{dc_l}{dt} = -\frac{S_\delta a}{V_c} j'_z, \quad \frac{dc_u}{dt} = +\frac{S_\delta a}{V_c} j'_z \quad (25)$$

Here S_δ denotes the cross sectional area of the channel. In the initial stage of separation until the concentration difference $\Delta c = c_l - c_u$ is significantly less than the initial concentration c_0 , the particle flux may be calculated assuming that the concentration profile across the channel is time dependent but does not depend on the vertical coordinate z , $c = c(x, t)$.

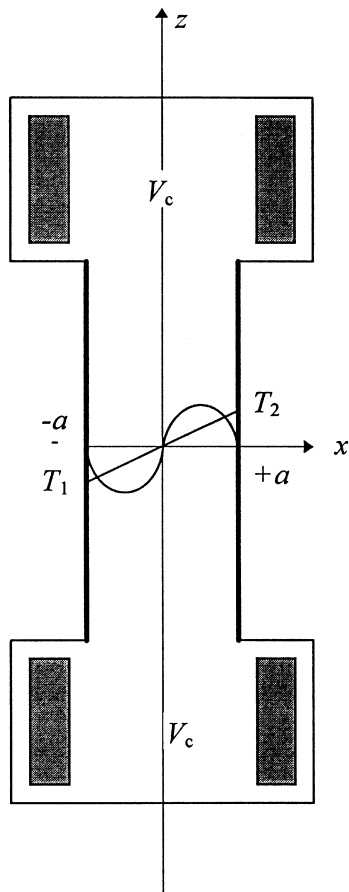


Fig. 6. The sketch of the thermal diffusion column. The induction coils of the LC oscillator (the gray areas represents their cross section) for particle concentration measurements are mounted in the upper and lower separation chambers.

Using the unsteady particle flux for $\alpha \rightarrow 0$ in the form of Eq. (13), we obtain from Eq. (25) the following relation which describes the development of the concentration difference Δc in the initial regime of separation:

$$\frac{\Delta c}{c_0} = -\frac{kGr_T Sc}{5400} \frac{\delta}{L_c} n^5 \left[\left(1 - \frac{5n}{6} + \frac{10n^2}{49} \right) + S \left(\frac{25n^2}{63} - \frac{n^3}{4} \right) \right] \quad (26)$$

(The thermal and the concentration Grashoff numbers Gr_T and Gr_c as well as the boundary layer thickness $n = (12\tau)^{1/2}$ and the diffusion Fourier number $\tau = Dt/\delta^2$ here and below are calculated using the channel thickness $\delta = 2a$, $L_c = V_c/S_\delta$ is the effective length of the upper and lower separation chambers).

This dependence is valid for $\tau < 1/48$ until the thickness of the concentration boundary layers from both walls reaches the center of the channel at $n = 0.5$. From Eq. (26) it follows that in the initial regime of separation a nonlinear dependence $\Delta c \sim \tau^{2.5}$ is awaited. Even at high values of the parameter $S = k(Gr_c/Gr_T)$ the influence of the concentration buoyancy force on the separation dynamics in this regime is relatively low.

At $\tau > 1/48$ the concentration profile across the channel starts to saturate and approximately at $\tau \approx 0.25$ a steady profile (Eq. (5)) is reached. Now, the vertical particle flux becomes constant and the concentration difference starts to develop linearly in time. For small values of k ($k < 1$) when the steady concentration distribution across the channel is linear, we obtain

$$\frac{\Delta c}{c_0} = +\frac{2}{6!} \frac{\delta}{L_c} kGr_T Sc(1+S)\tau. \quad (27)$$

At durable separation, starting after a certain transition time τ_t (from our previous analytical results [10] it follows that $\tau_t \approx 65(Gr_T Sc \delta / L_c)^{-1}$ the concentration difference in the chambers starts to saturate and the linear dependence (Eq. (27)) may not be observed. The smaller the volume of separation chambers V_c or the higher the temperature difference ΔT , the sooner the linearity of the saturation curves vanishes. In the transition regime a time interval exists in which the concentration difference $\Delta \varphi$ may be approximated by a square-root dependence [10]

$$\frac{\Delta c}{c_0} = \gamma \frac{L}{L_c} k \sqrt{\tau} \quad (28)$$

The coefficient γ slightly depends on the ratio L/L_c . For devices having approximately equal volumes of

the active column V and of the upper and lower containers $V_{c,\gamma} \approx 0.619$ is found [7].

In long time experiments i.e. for some time τ_s (for $L/L_c \approx 1$ $\tau_s \approx 5 \times 10^7 (Gr_T Sc \delta / L)^{-2}$ [6]) a stationary regime of particle separation is reached. In accordance with Eq. (24) for liquids with $S \rightarrow 0$, the concentration difference in the column chambers in the asymptotic regime $\tau > \tau_s$ is

$$\frac{\Delta c}{c_0} = 504 \frac{k}{Gr_T Sc} \frac{L}{\delta} \quad (29)$$

From the results presented in Fig. 5, it is seen that the concentration buoyancy force starts to affect the steady separation level in the column if the parameter S exceeds a value approximately equal to 2. In both cases of positive and negative values of S an increase of the steady concentration difference takes place.

Fig. 7 represents some results of a computer simulation of the unsteady particle separation problem in a column for parameters which are close to our experiments [11]. Numerical results confirm the '5/2' law $\Delta C \sim \tau^{5/2}$. It is seen that at $S = 0$ the approximation (26) is valid till $\tau < \tau_1 \approx 0.025$ before the concentration boundary layers on both walls reach the center of the channel.

Usually, in real separation devices, the column width is varied within an interval of about $\delta = 0.5\text{--}1$ mm and the thermal as well as the concentration Grashoff

numbers reach values 1–10. Besides, for colloidal particles in ferrocolloids the values of the Schmidt number Sc are very high ($Sc \approx 10^5$). The time at which the steady separation regime is reached, depends on the convection parameters as well as on L and L_c . In our experiments the relaxation time $t_s = \tau_s \delta^2 / D$ exceeds several tens of hours. To simplify the measurements as well as to eliminate the difficulties of separation curve analysis due to not very well clarified concentration convection effects, the main attention in our experiments is paid to the nonstationary regime of the particle separation curves.

6. Experimental results

The separation experiments are performed using a vertical flat column of width $\delta = 0.52$ mm and of height $L = 86.5$ mm. The heated and cooled walls are connected with two precise thermostats, keeping the temperatures T_2 and T_1 constant. The difference $\Delta T = T_2 - T_1$ is varied in the interval 2–18°C. In order to lower the temperature inhomogeneities caused by heat exchange with the environment, the upper and lower containers of equal volume ($V_c \approx 1$ cm³) and the outside walls of the channel are made from plastic material with a low heat conductivity. The column is located between poles of an electromagnet in a region of uniform magnetic field.

Particle concentration in both separation chambers is determined by measuring the resonance frequency of an LC oscillator [2]. The inductance coils of the oscillator are mounted inside the both containers (see Fig. 6). In the presence of an increasing magnetic field H when according to the superparamagnetic nature of magnetic colloids the differential magnetic susceptibility monotonously decreases, a reduction of the resonance frequency sensitivity to the particle concentration takes place. Therefore, the concentration measurements are performed accounting for the effect of a magnetic field on the graduation curves of the oscillator.

The separation measurements are performed employing tetradecane based ferrofluid samples containing chemically coprecipitated magnetite or Mn–Zn ferrite nanoparticles. The colloids are stabilized by using oleic acid as a surfactant. The magnetization M of the colloids obeys the Langevin law $M = \phi M_p (\coth \xi - 1/\xi)$ with $\xi = \mu_0 m H / k_B T$. Here k_B is the Boltzmann constant and μ_0 is the magnetic constant. The physical characteristics of a ferrofluid containing Fe₃O₄ particles (sample 1) are as follows: the volume fraction of the magnetic particles $\phi = 0.037$ (determined from fluid density measurements), their magnetic moment $m = 1.4 \times 10^{-19}$ A/m² (deter-

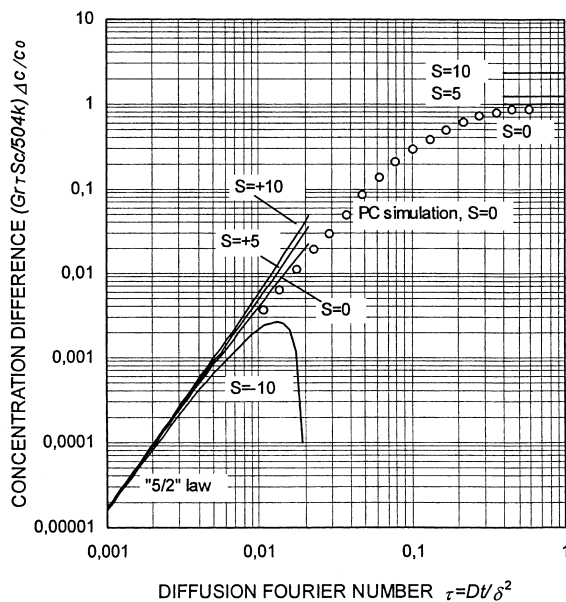


Fig. 7. Unsteady particle separation curves in the column of $L_c/L = 1.2$, $Ra_T = 3$, $Sc = 10^5$. Lines represent the analytical solution (26) for the region of low τ and (17) at $\alpha = 0$ for the saturated regime. Dots represent the results of a numerical solution [11].

mined by a magnetogrulometry analysis [12]), $d = 8.2$ nm (a ‘magnetic’ diameter calculated using the assumption that the saturation magnetization of the particle material M_p is equal to that of bulk magnetite, $M_p = 480$ kA/m), $\eta = 4.6 \times 10^{-3}$ N s/m², $\beta_T = 8.3 \times 10^{-4}$ K⁻¹, $\beta_\varphi = 5.9$. The corresponding parameters of the Mn–Zn ferrite particles (Mn_{0.5}Zn_{0.5}Fe₂O₄) containing fluid (sample 2) are: $\varphi = 0.0928$ (initial sample), $m = 2.22 \times 10^{-19}$ A/m², $M_p = 249$ kA/m, the ‘magnetic’ diameter $d = 12$ nm, kinematic viscosity $\nu = 26.6 \times 10^{-6}$ m²/s (initial sample, $T = 25^\circ\text{C}$) and $\nu = 3.3 \times 10^{-6}$ m²/s (sample diluted to 1:4) [12].

Several series of separation experiments have been performed to evaluate the thermal diffusion ratio in a zero magnetic field. Fig. 8 represents the nonstationary separation curves of lyophilized Mn–Zn ferrite particles dispersed in tetradecane [13]. The measurements are performed employing the initial sample 2 and a fluid of relatively low particle concentration (the initial sample diluted to 1:4), the temperature difference is $\Delta T = 10^\circ\text{C}$. We can see that experimental results confirm both the dependence $\Delta c/c_0 \sim t^{5/2}$ predicted by Eq. (26) (initial regime, $t < 800$ s) and the empirical relation indicated by Eq. (28) (starting after approximately 2000 s). The difference in the separation rates for both samples at low τ reflects the effect of the fluids viscosity (ν of the diluted sample is 8 times lower than that of the initial sample) on the convection intensity.

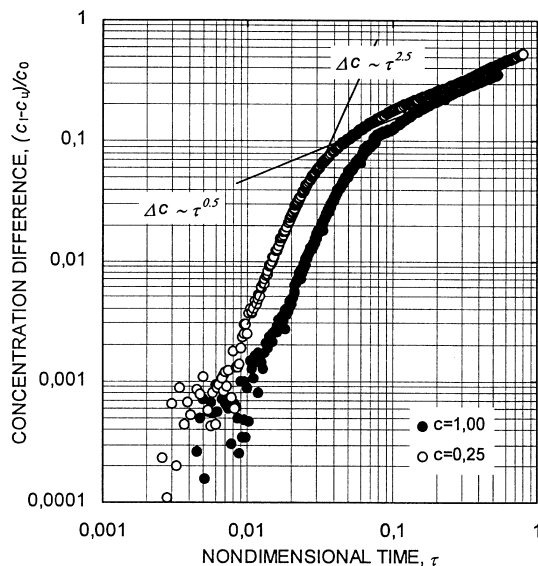


Fig. 8. The unsteady particle separation in a vertical column. Mn_{0.5}Zn_{0.5}Fe₂O₄ particles stabilized by oleic acid. Initial, $\varphi = 9.3 \times 10^{-2}$ (marked as $c = 1$), and diluted, $\varphi = 2.3 \times 10^{-3}$ ($c = 0.25$), samples, $\Delta T = 10^\circ\text{C}$.

Analyzing the particle separation curves of the series of experiments we come to the conclusion that the thermal diffusion ratio $\alpha_T = S_T T$ neither depends on particle concentration nor on temperature difference [2]. The average value α_T for Fe₃O₄ particles calculated from the initial part of the separation curves (accounting only for the first summand in Eq. (26)) is $\alpha_T = +24 \pm 5$. From an analysis of the results using Eq. (28) a practically identical result is obtained, $\alpha_T = +21 \pm 4$ [7]. For Mn–Zn ferrite particles the corresponding α_T values are a little lower: $\alpha_T = +13.8 \pm 1.3$ (the ‘5/2’ law) and $\alpha_T = +18.3 \pm 0.2$ (the ‘1/2’ law) [13]. The measured positive values of the Soret coefficients for surfacted particles agree qualitatively well with theoretical predictions [14]. To analyze the results quantitatively, it is necessary to note that the convection parameters which are used to evaluate the S_T value are not very well determined. The Schmidt number Sc is calculated in the Stokes approximation $D = kT/(3\pi\eta d)$ employing the ‘magnetic’ diameter of particles and assuming that the thickness of the surfactant layer around the particle is equal to 2 nm. Some preliminary diffusion measurements show that such calculation is not very precise. For example, for the diluted Mn–Zn ferrite containing sample it is found from dynamic optical grating experiments that $D = 7.4 \times 10^{-13}$ m²/s [15], which is remarkably less than the value obtained theoretically by using the Stokes approximation.

An external magnetic field oriented horizontally along the isothermal walls of the channel ($B \perp \nabla T$) causes an increase in the separation intensity of the surfacted particles whereas in the presence of B oriented transversally to these walls ($B \parallel \nabla T$) a remarkable reduction of the vertical particle flux is observed. Fig. 9 presents the thermophoretic mobility of Fe₃O₄ and Mn_{0.5}Zn_{0.5}Fe₂O₄ nanoparticles under the effect of a uniform field $B \perp \nabla T$ [6] and $B \parallel \nabla T$ [13]. Due to a low electrical conductivity of the hydrocarbon-based colloids it can be assumed, that in these experiments $a \ll 1$. Therefore, the dots represent average values of results calculated using the expressions (26) and (28), assuming that only particle thermal diffusion is affected by a magnetic field. Both effects, the increase in α_T in the presence of a transversal field $B \perp \nabla T$ and the approximately two times stronger reduction of α_T if $B \parallel \nabla T$, agree well with the hydrodynamic theory [16]. Nevertheless, the magnetic effects presented in Fig. 9 are stronger than the theoretically predicted ones. Obviously, if thermodiffusive transfer of nanometer scaled particles is analyzed, the hydrodynamic theory must be specified taking into account a slip velocity and a temperature jump on the particles’ solid–liquid interface.

A magnetic field may also influence the particles’ diffusivity and the fluids’ viscosity. From the hydrodynamic theory [16] as well as from a thermodynamic

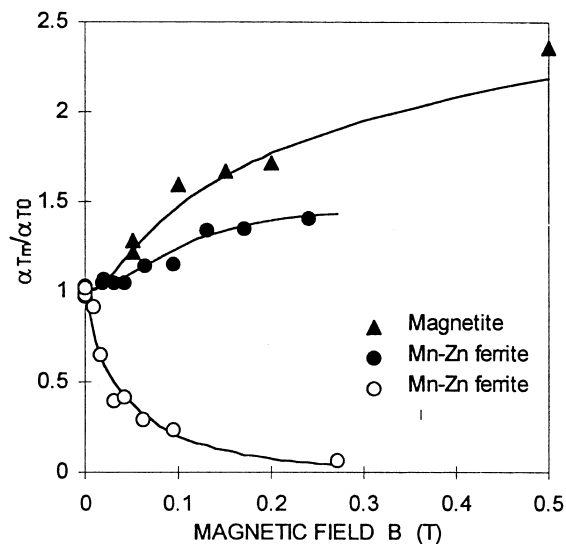


Fig. 9. The effect of a magnetic field on the Soret coefficient of surfacted magnetite (triangles) and Mn–Zn ferrite (dots and circles) particles in tetradecane. Black points: $B \perp \nabla T$, white points: $B \parallel \nabla T$.

analysis accounting for particle interactions [17] it follows that a magnetic field oriented along the concentration gradient causes an increase of the translation diffusion, whereas in the presence of a transversal field $B \perp \nabla T$ a reduction of D is awaited. Optical grating experiments confirm both of these ‘magnetodiffusivity’ effects [17]. Nevertheless, if a change of the particle mass diffusion coefficient in our experiments really takes place, the corresponding analysis of the separation curves by using the corrected coefficients in Eqs. (26) and (28) would give the thermomagneto-phoretic effect even stronger than that presented in Fig. 9. We expect that the second effect, the fluid ‘magnetoviscosity,’ does not significantly influence particle separation dynamics in the column because the measurements are performed using colloids of a relatively low particle concentration. More significant seems to be a possible magnetorheological behavior of the colloidal systems if strong particle interactions are present. For example, in some preliminary experiments performed using water-based colloids which contain charged particles (‘ionic’ ferrofluids) we observed a significant reduction of particle separation in a magnetic field independently of the orientation of B to the temperature gradient ∇T . A magnetohydrodynamic breaking of convection may not give so strong an effect since not only in hydrocarbons but also in electrolytes the Hartmann number is low (in the examined ionic fluid the α even in strong fields does not exceed the value 0.2).

7. Conclusions

The particle separation measurements in a vertical thermal diffusion column has been used to evaluate the Soret coefficient of colloidal magnetic particles in ferrofluids. To interpret the results, the thermal diffusion theory is modified by taking into account the concentration buoyancy force arising during the separation of particles and the MHD breaking of convection in a channel. Experiments confirm the analytically predicted ‘5/2’ law of the unsteady separation curves. Colloidal ferrite particles in hydrocarbons stabilized by use of surfactants are moving towards lower temperatures. This direction of thermophoresis agrees well with the predictions of the thermodynamic theory accounting for a slip velocity of lyophilic solid–liquid boundaries. Experiments confirm the theoretically predicted effect of a uniform magnetic field on the thermophoretic transfer of nanoparticles in ferrofluids and the anisotropy of the magnetic Soret effect. Hartmann’s type MHD effects in thermal diffusion column experiments using both the lyophilized and the electrically stabilized magnetic fluids may be neglected. Additional separation experiments would be interesting to perform to investigate the convection stability under the effect of a negative Soret coefficient. Some theories predict that $S_T < 0$ may be observed in ionic ferrofluids containing charged particles. It is necessary also to investigate the critical conditions of thermomagnetic instability of the convective shear flow in the presence of a strong magnetic field $B \parallel \nabla T$.

Acknowledgements

The authors are thankful to our colleague A. Mezulis for performing the separation measurements. The work has been financially supported by the Latvian Science Council (Grant 96.0271) and the German Ministry of Education and Science, BMBF (Grant LET-001-96).

References

- [1] S. Van Vaerenbergh, S.R. Coriel, G.B. McFadden, B.T. Mutay, J.C. Legros, Modification of morphological stability of Soret diffusion, *J. Crystal Growth* 147 (1995) 207–214.
- [2] A. Mezulis, E. Blums, G. Kronkalns, M. Maiorov, Measurements of thermodiffusion of nanoparticles in magnetic colloids, *Latvian Journal of Physics and Technical Sciences* 5 (1995) 37–50.
- [3] J. Langlet, Generation de second harmonique et diffusion Rayleigh forcee dans les colloides magnetiques,

- Ph.D. thesis, de l'Universite Paris 7 Denis Diderot, Paris, 1996.
- [4] G.D. Rabinowich, R.J. Gurevich, G.I. Bobrova, *Thermodiffusion Separation in Liquid Dispersions*, Nauka i Tehnika, Minsk, 1971 (in Russian).
- [5] O. Ecenarro, J.A. Madariaga, J. Navarro, C.M. Santamaria, J.A. Carrion, J.M. Saviron, Non-steady density effects in liquid thermal diffusion columns, *J. Phys.: Condens. Mater* 1 (1989) 9741–9746.
- [6] E. Blums, A. Mezulis, Thermal diffusion and particle separation in ferrocolloids, in: A. Alemany, Ph. Marty, J.R. Thibault (Eds.), *Transfer Phenomena in Magnetohydrodynamic and Electroconducting Flows*, Kluwer Academic Publishers, Dordrecht, Boston/London, 1999, pp. 1–16.
- [7] E. Blums, A. Mezulis, M. Maiorov, G. Kronkalns, Thermal diffusion of magnetic nanoparticles in ferrocolloids: experiments on particle separation in vertical columns, *J. Magn. and Magn. Materials* 169 (1997) 220–228.
- [8] O. Ecenarro, J.A. Madariaga, C.M. Santamaria, M.M. Bou-Ali, J.J. Valencia, Influence of the Grashoff number on the stability of the thermogravitational effect in mixtures with negative thermal diffusion factors, in: *Proceedings of the Third International Meeting on Thermodiffusion*, University Mons-Hainaut, Mons, 1998, pp. 118–122.
- [9] O. Ecenarro, J.A. Madariaga, C.M. Santamaria, M.M. Bou-Ali, J. Valencia, Diffusion thermogravitacionnelle dans des melanges liquides a effet Soret negatif, *Entropie* 32 (198/199) (1996) 71–76.
- [10] E. Blums, G. Kronkalns, R. Ozols, The characteristics of mass transfer processes in magnetic fluids, *J. Magn. and Magn. Materials* 39 (1983) 142–146.
- [11] E. Blums, A. Savickis, Convection in thermomagnetic diffusion column: unsteady effects caused by particle transfer in ferrofluids, in: *The Fourteenth International Riga Conference on Magnetohydrodynamics MAHYD'95*, August 24–26, IOP, Riga, 1995, p. 167.
- [12] M.M. Maiorov, Magnetization curve of magnetic fluid and distribution of magnetic moment of ferroparticles, in: *Proceedings of Tenth Riga MHD Conference*, IOP, Salaspils, vol. 1, 1981, pp. 11–18.
- [13] E. Blums, S. Odenbach, A. Mezulis, M. Maiorov, Soret coefficient of nanoparticles in ferrofluids in the presence of a magnetic field, *Physics of Fluids* 10 (9) (1998) 2155–2163.
- [14] J.L. Anderson, Colloidal transport by interfacial forces, *Ann. Rev. Fluid Mech* 21 (1989) 61–96.
- [15] A. Mezulis, private communication.
- [16] E. Blums, Some new problems of complex thermomagnetic and diffusion driven convection in magnetic colloids, *J. Magn. and Magn. Materials* 149 (1995) 111–115.
- [17] J.-C. Bacri, A. Cebers, A. Bourdon, G. Demouchy, B.M. Heegard, B.M. Kashevsky, R. Perzynski, Transient grating in a ferrofluid under magnetic field. Effect of magnetic interactions on the diffusion coefficient of translation, *Phys. Rev. E* 52 (1995) 3936–3942.